Journal of Advances in Nanomaterials, Vol. 2, No. 3, September 2017
https://dx.doi.org/10.22606/jan.2017.23004

Spectroscopic Investigation on Sol Gel Derived TiO_2 Nanoparticles

Praveen Kumar Singh[1*], Soumya Mukherjee[2], Chandan Kumar Ghosh[3], Saikat Maitra[1]

[1] Government College of Engineering and Ceramic Technology, Kolkata -10, India
[2] Amity school of Engineering and Technology, Amity University, Kolkata, India
[3] School of Materials Science and Nanotechnology Jadavpur University, Kolkata, India
Email: pksingh166@gmail.com

Abstract. TiO_2 nanoparticles were synthesized by sol-gel method from titanium tetra isopropoxide. Influence of heat treatment on structural and morphological properties of TiO_2 nanoparticles was investigated by XRD and SEM. Spectral properties of the nanoparticles were investigated using FTIR, Raman spectroscopy, PL spectroscopy and UV–visible absorption spectroscopy. XRD analysis revealed the formation of mixed anatase and ruitle phase in the synthesized powder at 550°C and existence of only rutile phase at 750 and 900°C. The lattice parameters, crystallite sizes, volume of the unit cell, density and surface area of TiO_2 nanoparticles were determined from XRD analysis. SEM analysis showed that the prepared nanoparticles were in the nano regime, nearly spherical and larger agglomerated at lower temperature. EDX analysis showed that the TiO_2 composition obtained was near stoichiometric at lower temperature and the proportion of oxygen vacancy increased with the increase in temperature. The presence of Ti-O and Ti-O-Ti bonds was confirmed by FTIR spectra. PL spectroscopy showed that the change in surface states and presence of anatase and rutile phases of TiO_2 were also responsible for exhibiting the change in PL intensity. UV–visible absorption spectra showed the shifting of absorption edge towards the higher wavelength with the increase in temperature while the corresponding energy band gap of semiconductor nanoparticles decreased. Change in Raman spectra with the increase in temperature was observed due to anatase to rutile phase transformation and with the increase in the particle size.

Keywords: TiO_2 nanopowder, sol-gel, annealing, spectroscopic properties.

1 Introduction

Titania nanoparticles have important applications in the field of optical devices, sensor and photocatalysis [1, 2]. These nanoparticles have different electrical, optical and magnetic properties compared to their bulk counterparts due to large surface to volume ratios and quantum size effect [3]. There are several factors in determining the important properties like, particle size, crystallinity and morphology that affect the performance of TiO_2 in applications [4-6]. TiO_2 as a wide indirect band gap n-type semiconductor and generally exist in the three polymorphs of TiO_2 are anatase (I4/amd), rutile (P42/mnm) and brookite (Pcab). Brookite exists in an orthorhombic structure while anatase and rutile both possess tetragonal unit cells. Among these, anatase is metastable at lower temperature and has excellent chemical and physical properties for environmental purification, although rutile is the more stable phase from thermodynamic point of view. The phase composition has significant effect on the properties and performance of nano TiO_2 and therefore it is desirable to control the transformation to develop a particular phase or phase mixture subsequent to thermal treatment. The phase transformation depends on the growth process affected by defect concentration, grain boundary concentration and particle packing as well [7-9].

The final properties of the nano TiO_2 are naturally dependent on the method of synthesis, the experimental conditions and the structure of the polymorph. Different techniques have been used for the preparation of TiO_2 nanoparticles, which include sol–gel, different forms of sputtering from metallic and ceramic targets, electron beam evaporation, pulsed laser deposition and chemical vapour deposition. Considering the advantages and disadvantages of these methods, sol-gel process has been chosen as the

most important process because of its low reaction temperature, narrow range of particle distribution, controllable particle-size, low cost and ease of processing for the preparation of TiO_2 nanoparticles [10].

In the present work, TiO_2 nanoparticles were synthesized by sol-gel method, which was followed by calcination of the gel at three different temperatures. The structural transformations by XRD and related optical changes in UV-Vis, photoluminescence, FTIR and Raman spectrum of TiO_2 have also been studied.

2 Experiment

For the synthesis of TiO_2 sol from alkoxide precursor, 10ml titanium (IV) isopropoxide $Ti[OCH(CH_3)_2]_4$ (SIGMA-ALDRICH), 3ml Diethanolamine (DEA) $C_4H_{11}NO_2$ (MERCK) and 60ml ethanol $[C_2H_6O]$ (MERCK) were taken as the starting materials. The required volume of ethanol was mixed with diethanolamine (DEA) and then titanium isopropoxide was added to it slowly; this mixture was vigorously stirred for 40 minutes, with the addition of 1 ml of water. The sol was observed to be stable for 7 days and then it was transformed to gel. The stability of the sol also increased with the decrease in the humidity. In the course of drying, the volume of the sol decreased to eleven fold with the formation of a shrinked xerogel by evaporation. The gel was heat treated at different temperatures ca, 550, 750 and 900°C for 1h in an electrically heated muffle furnace with heating rate of 5°C/ minute.

All the samples were characterized by X-ray diffraction (XRD) [Model Regaku ultima-III], The grain size of the samples was calculated using Scherrer equation [11] as given below

$$D = 0.94\lambda \,/\, \beta Cos\theta \tag{1}$$

where: D is size of crystallite, λ is wave length, β is FWHM, θ is angle

The individual contributions of crystallite sizes and lattice strain on the peak broadening of the TiO_2 nano particle analysis by using size-strain plot of Williamson–Hall (W–H) method [12, 13].

$$(\beta Cos\theta) \,/\, \lambda = 1 \,/\, D \; + \eta(Sin\theta \,/\, \lambda) \tag{2}$$

where β is FWHM in radians, λ is the wavelength of X-ray, θ is the diffraction angle, D is the effective particle size and η is the effective strain.

In the W-H plot between βcosθ/λ and sinθ/λ for the prepared samples, negative slope in the plot indicates the presence of compressive strain [14] whereas the positive slope indicates the presence of tensile strain [15].

The X-ray density has been calculated for the samples by using equation (4) [16, 17].

$$\rho = nM \,/\, NV \tag{3}$$

where M is the molecular weight, N is Avogadro's number and V is the volume of unit cell. For anatase phase n is four and for rutile phase n is two [18].

Further, the specific surface area is calculated by the equation (4) [17].

$$S_a = 6 \,/\, D\rho \tag{4}$$

where D is crystallite size and ρ is the density.

Scanning electron microscopy (SEM) [Hitachi Model S-4800] was carried to observe the morphological changes. Optoelectronics behavior of the material was determined by Fourier transform infrared spectroscopy (FTIR) [Prestige spectrophoto meters Model -21], ultraviolet visible spectroscopy (UV-Vis) [Perkin Elmer, Model Lambda 35], Raman spectroscopy [Witec alpha Model 330R] and photoluminescence spectroscopy (PL) [Elico Model Sl-174].

3 Results and Discussion

From the XRD diffraction study (Fig. 1) of alkoxide derived TiO_2, it was observed that at 550°C, the sample contained anatase as the major crystalline phase. The characteristics lattice planes of anatase (101), (004), (200), (211), (105) were observed with high intensities and (110), (101), (111), (211), (220), (301) planes of rutile were also detected in the sample. With increasing temperature the proportion of rutile phase in the sample increased significantly. The relative rutile phase was calculated using the equation given below [19].

$$W_r = I_r \,/\, \left(\left(0.884 I_a + I_r\right)\right) \tag{5}$$

where, W_r is the rutile weight %, I_r is intensity of (110) peak of rutile and I_a is intensity of (101) peak of anatase.

It was observed that at 550°C about 28% rutile phase was present in sample. Although anatse and rutile have the same basic TiO_6 octrahedral, the arrangement of atoms in the basic unit changed when the rutile phase was developed during phase transformation from anatse to rutile. TiO_6 octrahedral underwent distortion on heat treatment and finally breaking and recombination of new Ti-O bonds took place at the interphase and at the grain interiors. Lattice distortion and breaking of Ti-O bonds at higher temperatures resulted in the removal of oxygen ions and creation of defects along with the development of new Ti-O bonds in the rutile phase.

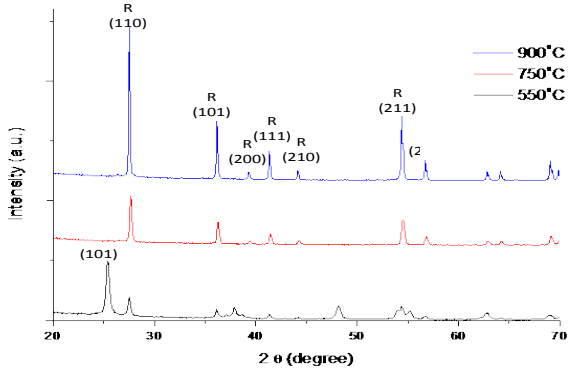

Figure 1. XRD profile of alkoxide derived TiO_2 at 900°C, 750°C and 550°C heat treatment temperature.

At 750°C all the peaks in the diffractogram corresponding to the rutile phase was noted, indicating the completion of phase transformation process by this temperature. The increase in intensities of all the characteristic planes (110), (101), (111), (211), (220) indicated final reconstruction of rutile phase with the removal of residual defects.

The % error in the intensities of diffraction was calculated by taking standard volume of anatse (135.25 Å) and for rutile (62.43 Å) from JCPDS No. 010731764 and 000040551. The % cell volume error is given in table 1.

Table 1: Structural parameter of TiO_2 nanoparticles (A-anatse, R- rutile).

Calculated parameters	**550°C**	**750°C**	**900°C**
FWHM (radian)	0.0062(A)		
	0.0045(R)	0.0034(R)	0.0022(R)
d- spacing (Å)	3.504 (A)		
	3.237 (R)	3.2211 R)	3.2395(R)
Unit cell volume (Å)	135.58 (A)		
	62.04 (R)	62.10 (R)	62.31 (R)
Volume % error	0.243 (A)		
	0.624(R)	0.528(R)	0.192 (R)
Size (nm) by (Sche. Eq.)	24.48	40.27	56.98
Size nm (W-H plot)	29.71	41.37	58.36
Strain η	0.02203	0.00537	0.00213
Density (g/cm^3)	4.014	4.271	4.257
Surface area S_a (m^2/gm) by (W-H plot)	50.31	33.95	24.15

For the alkoxide derived TiO_2 powder, it was observed that the grain size increased as a function of heat treatment. These grain growths can be related to the removal of oxygen vacancy and increasingly convex nature of the grain boundary. As a result of this the ions migrated towards the outer side and

the grains tend to grow thereby larger. The change in the chemical potential of the atoms across the curved grain boundary side acted as the driving force to move the boundary and resulted in the increase in the boundary [20-22].

It has been observed that with the increase in heat treatment temperature the particle sizes increased from 29.71 nm to 58.36 nm monotonically. Tensile strain values on the other hand decreased sharply after the heat treatment from 550 to 750°C and afterwards the reduction in the tensile strain was not much significant (Fig. 2). This may be related to the structural relaxation of the anatase from of crystallite to the equilibrium value progressively at elevated temperatures.

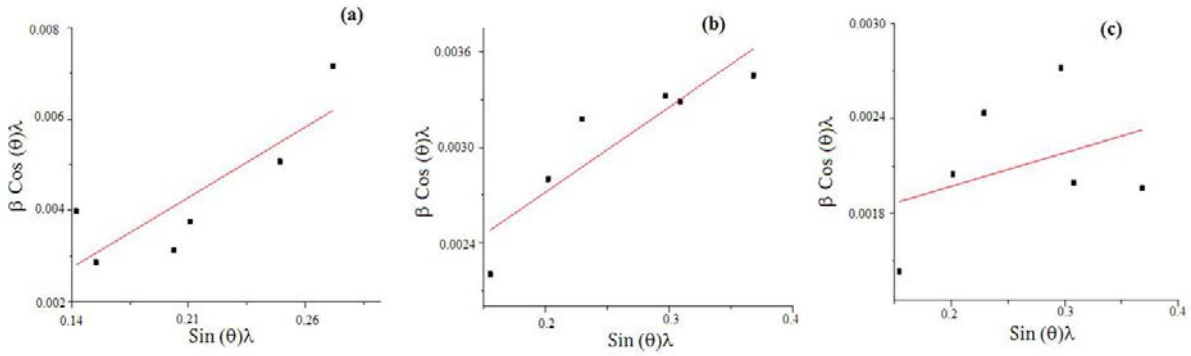

Figure 2. W-H plots of alkoxide derived TiO_2 at (a) 550°C, (b) 750°C and (c) 900°C heat treatment temperature.

SEM micrograph (Fig. 3) of the alkoxide precursor derived TiO_2 the consisted of nano sized primary particles with spherical shape and the larger agglomerates proportion of the particles were detected in pure TiO_2. Increase in the particle size with calcination temperature can be related to the crystal growth and change in the dispersion behavior of the agglomerates as a function of temperature was noticed in the micrographs.

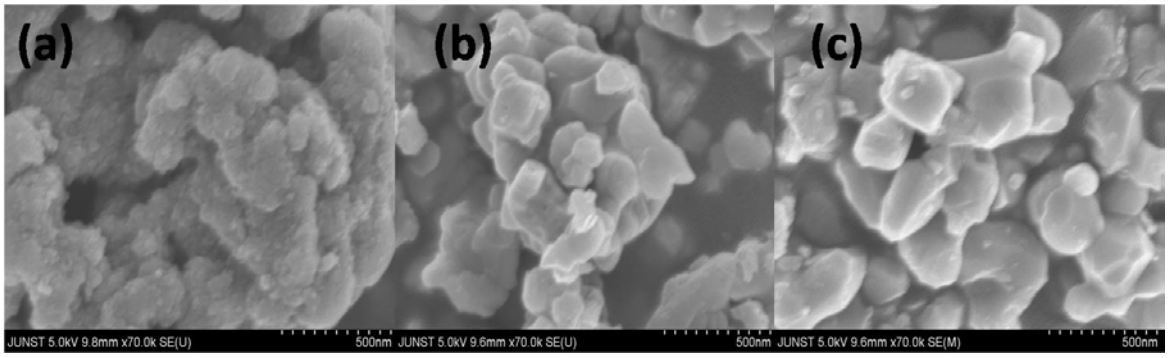

Figure 3. SEM micrographs of alkoxide derived TiO_2 at (a) 550°C, (b) 750°C and (c) 900°C heat treatment temperature.

From EDX analysis, it has been observed that with increase in the calcination temperature, the proportion of oxygen atoms decreased from 38.33 to 27.62 At% and the proportion of Ti in TiO_2 increased for the alkoxide derived precursors. It indicates that, with the increase in the calcination temperature, oxygen ions came out of the structure with the formation of oxygen vacancies.

After heat treatment at 550°C, the vibrations ν(Ti-O) and ν(Ti-O-Ti) modes were observed at 400-800 cm^{-1} wave number region (Fig. 4). It is the characteristics stretching vibration zone of ν(Ti-O) indicating the formation of more and more (Ti-O) stretching bonds in the structure as a result of the removal of volatile from it due to the heat treatment.

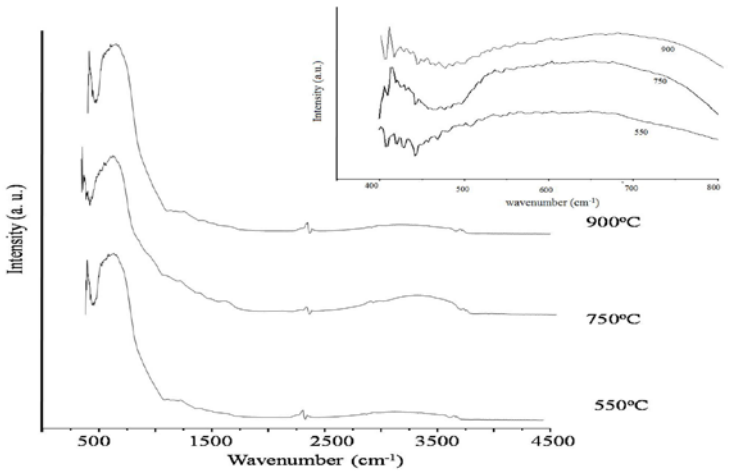

Figure 4. FTIR spectra of alkoxide derived TiO_2 at 550°C, 750°C and 900°C heat treatment temperature.

Appearance of small band at 1341cm^{-1} was related to the symmetric deformation of CH_3 group from the isopropoxide and it indicated the presence of trace amount of isopropoxide in the structure. The trace amount of alkoxide also produced small peak at 2902cm^{-1} which was in between the symmetric and asymmetric stretching mode of CH_2 of alkoxide group. Peak at 3294cm^{-1} was related to the symmetric stretching vibration of Ti-OH group and the corresponding bending vibration was observed at 1624cm^{-1} indicating the relatively higher energetic existence of the bonded -OH group.

For heating to 750°C all the peaks related to ν(Ti-O-Ti) stretching vibration were retained in the structure. These peaks were 405cm^{-1}, 413cm^{-1}, 426cm^{-1}, 429cm^{-1}, 435cm^{-1} and 440cm^{-1}. The elimination of the peak at 502cm^{-1} and 565cm^{-1} compared to the sample heated at 550°C indicated an occurrence of the change in the nature of Ti-O bond which can be related to the progressive phase transformation from anatase to rutile phase. It is also supported by a significant enhancement in the absorbance of the ν(Ti-O-Ti) vibration. Increasing number of stretching vibration of Ti-O-Ti band suggest that after heating at 550°C and 750°C the onset of the constrictive process towards the formation of TiO_2 lattice from the precursor. As a result of heat treatment the organic part -[$OCH(CH_3)_2$] of the precursor was not only getting dissociated from the structure of the precursor with the formation of volatile but also resulted in the formation of unoxidized traces. Appearance of the bands as at 2348 and 2388cm^{-1} indicated the formation of dehydrogenated as well as unoxidized carbon base precursors. The appearance of very small bands at 2902cm^{-1} and 2987cm^{-1} indicated the presence of entrapped residual alkoxide in the structure, as the band indicated existence of CH_2 stretching mode. After heating at 900°C the number of band around 400-700cm^{-1} decreased in number and slightly changed from their previous position indicating a qualitatively change in ν(Ti-O-Ti) stretching vibration. It supported the fact of complete phase transformation of anatse to rutile.

The Raman spectra of the alkoxide derived sample heated at 550°C showed low intensity peaks for anatase 408 cm^{-1} (B_{1g}), 526 cm^{-1} (B_{1g}), 652 cm^{-1} (E_g) and for rutile phase one high intensity peak corresponding to (E_g) 156 cm^{-1} was observed (Fig. 5). Lattice strain defects and crystallite sizes have a profound influence in the peak shift, peak broadening and intensity of the Raman peaks.

After heating at 750°C the appearance of the Raman peak at 244 cm^{-1} can be related to the compound vibration as a result of multiple phonon scattering process [23]. Only Raman peaks corresponding to the rutile phase were observed here at 460 cm^{-1} (E_g) and 620 cm^{-1} (A_{1g}). All the detected peaks were of the medium intensities.

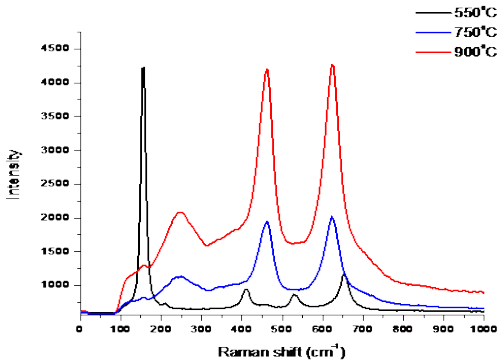

Figure 5. Raman spectra of alkoxide derived TiO_2 at 550°C, 750°C and 900°C heat treatment temperature.

The peak corresponding to E_g and A_{1g} modes of rutile vibration were observed in the sample heat treated at 750°C and 900°C [24]. But the relative error in the intensity of the peaks increased as the heating temperatures increased indicating completion in the formation of rutile phase at 900°C with elimination of defects on the crystal structure.

With 250 nm excitation wavelength electronic transition from the highest occupied molecular orbital to the lowest unoccupied molecular orbital will happen for TiO_2 developed from alkoxide precursor. PL emission peak was observed for the sample calcined at 550°C at 393nm but with the increase in calcination temperature the intensity of the emission peaks was reduced. The reduction in intensity with the increase in the calcination temperatures can be related to the generation of hole pair in the sample as the result of thermally assisted diffusion of ions in the lattice. The hole pair can interact with the electronic states generated in the forbidden gap in the TiO_2 thereby causing a reduction in the number of the field assisted transitions from the lower energy level to the higher energy level [25].

After calcination at 550°C with excitation of 320 nm three different peaks in the PL spectra were observed at 394 nm, 423 nm and 537 nm (Fig. 6b). After calcination at 750°C, with excitation of 320 nm the peaks were observed at 424, 466, 490 and 535nm. The peak at 394nm can be related to the transition from Ti^{+4} 3d states to O^{2-} 2p states. The peak at 432 nm can be related to the transition from Ti^{+4} 3d states to deep acceptor level OH^- and the peak at 537nm can be related to the transition from deep donor level created by O vacancy to the ground state for O^{2-} 2p states [25].

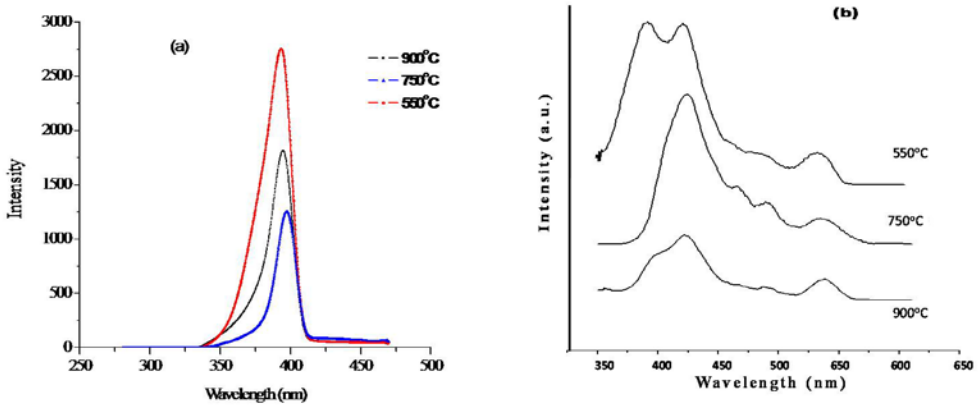

Figure 6. PL spectra at (a) 250 and (b) 320 excitation of alkoxide derived TiO_2 at 550°C, 750°C and 900°C heat treatment temperatures.

The significant low intensity of peak at 537 nm can be ascribed to relatively low concentration of O vacancy present in the system. With the increase in the calcination temperatures to 750°C only peaks at

424, 466, 489.5 and 535 nm were observed. Decrease in the relative intensity of the peaks can be related to the decrease in the surface states. As particle size increased from 29.71 nm to 41.37 nm with the increase in the calcination temperatures from 550°C to 750°C, it was revealed that more number of transitions to deep acceptor levels indicated the creation of more energy states at the acceptor level. Further there was phase transition from anatase to rutile and as a result of which the peak at 394 nm disappeared at 750°C. After calcining at 900°C the intensity of the peak at 538.5 nm became prominent indicating creation of deep doner level associated with O vacancy in the sample.

Generally the absorption edge in the case of TiO_2 nanoperticle is observed around 400 nm. Shifting of this absorption edge to lower wave length can be related to quantum confinement effect of nanoparticles, but other factors like effect of doping, particle size, relative proportion of rutile and anatase phases, defects from the crystal system etc. are also responsible for this phenomenon. These factors caused the irregular change in the absorption edge and band gap value of TiO_2 nanoparticle. Broad intense absorption of TiO_2 nano particles around 400 nm occurred due to the charge transfer from the valence band (here formed by 2p orbitals of the oxide anions) to the conduction band (here formed by 3d (Tg) orbital of the Ti^{+4} cations).

For alkoxide derived TiO_2 the calculated value of band gap was 3.44-3.08 eV in the temperature range of 550-900°C. With the increase in temperature red shift was observed. The complete transition from anatse to rutile phase at temperature 750°C resulted in some anomalous change in the UV absorption and band gap energy value of the sample. The incomplete crystallization on the surface roughness of the prepared samples in the formative stage could result in the development of considerable number of optical scattering center in the sample thereby affecting UV absorption and transmittance properties of sample.

With the increase in the calcination temperature, particle size of alkoxide derived TiO_2 increased and proportions of rutile phase also increased and the amount of lattice distortional defect also increased. A complicated interaction of these factors resulted in an irregular change (Fig. 7) in the absorption manner as well as band gap of the samples.

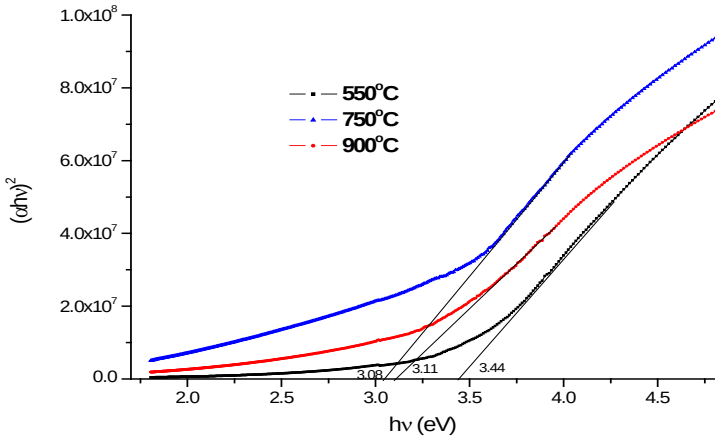

Figure 7. Tauc plots of alkoxide derived TiO_2 at 550°C, 750°C and 900°C heat treatment temperatures.

4 Conclusion

Titania nanoparticles were successfully synthesized by sol-gel method and calcinated at 550°C, 750°C and 900°C. From XRD analysis it was observed that TiO_2 nanoparticles consisted of anatase and rutile phase at 550°C with strain however, at higher temperature (750 and 900°C) only rutile phase was present in the samples. Calcination not only improved the crystallization of TiO_2 powders but also accelerated the phase transformation from anatase to rutile. The XRD result showed that the average crystallite size increased from 29.71 nm to 58.36 nm with the increase in temperature of TiO_2 and surface area decreased from 50.31 to 24.15 m^2/gm, which was consistent with the morphology observed

by SEM images. The TiO_2 nanoparticles at 550°C were nano sized primary particles with the larger agglomerates spherical shape. The optical band gap of TiO_2 nanostructures indicated the red shift with calcination temperature increased. Change in the pattern of Raman spectra was observed due to anatase to rutile phase transformation and with increase in particle size. The different peaks and change in intensity of PL spectra could be due to the recombination of photoinduced electrons and holes, oxygen vacancies, surface states and presence of anatase and rutile phases of TiO_2.

References

1. O. Harizanov and A. Harizanov, "Development and investigation of sol-gel solutions for the formation of TiO_2 coatings," *Solar Energy Materials and Solar Cells,* vol. 63, pp. 85-195, 2000.
2. B. Li, X. Wang, M. Yan and L. Li, "Preparation and characterization of nano-TiO_2 powder," *Materials Chemistry and Physics,* vol. 78, pp. 184-188, 2003.
3. H. Xu, X. Wang and L. Zhang, "Selective preparation of nanorods and micro-octahedrons of Fe_2O_3 and their catalytic performances for thermal decomposition of ammonium perchlorate," Powder Technology, vol. 185, pp. 176-180, 2008.
4. M. A. Behnajady, N. Modirshahla, M. Shokri, H. Elham and A. Zeininezhad, "The effect of particle size and crystal structure of titanium dioxide nanoparticles on the photocatalytic properties," *Journal of Environmental Science and Health,* vol. 43, pp. 460-467, 2008.
5. K. M. Lee, V. Suryanarayanan and K. C. Ho, "A Study on the Electron Transport Properties of TiO_2 Electrodes in Dye-Sensitized Solar Cells," *Journal of Power Sources*, vol. 188, pp. 635-639, 2009.
6. M. Ni, M. K. H. Leung, D. Y. C. Leung and K. Sumathy, "An analytical study of the porosity effect on dye-sensitized solar cell performance," *Solar Energy Materials and Solar Cells*, vol. 90, pp. 1331-1334, 2006.
7. D.A.H Hanaor and C.C. Sorrell, "Review of the anatase to rutile phase transformation," *Journal of Materials Science,* vol. 46, pp. 855-874, 2011.
8. D. Reidy, J.D. Holmes and M.A. Morris, "The Critical Size Mechanism for the Anatase to Rutile Transformation in TiO_2 and Doped-TiO_2" *Journal of the European Ceramic Society*, vol. 26, no. 9, pp. 1527–1534, 2006.
9. K.N.P. Kumar, K. Keizer, A. J. Burggraaf and H. Nagamoto, "Textural Evolution and Phase Transformation in Titania Membranes: Part 2.-Supported Membranes," *Journal of Materials Chemistry*, vol. 3, pp. 1151-1159, 1993.
10. N. B. Chaure, A. K. Ray and R. Capan, "Sol-Gel Derived Nanocrystalline Titania Thin Films on Silicon," *Semiconductor Science and Technology*, vol. 20, pp. 788-792, 2005.
11. D. Maheswari and P. Venkatachalam, "Sol-Gel Synthesis and Characterization of TiO_2 Nano Films in the Building of Dssc," *IOSR Journal of Electronics and Communication Engineering,* vol. 4, no. 4, pp. 29-33, 2013.
12. B. Choudhury and A. Choudhury, "Ce^{3+} and oxygen vacancy mediated tuning of structural and optical properties of CeO_2 nanoparticles," *Materials Chemistry and Physics*, vol. 131, no. 3, pp. 666-671, 2012.
13. G. K. Williamson and W. H. Hall, "X-Ray Line Broadening from Filed Aluminum and Wolfram," *Acta Metallurgica*, vol. 1, no. 1, pp. 22-31, 1953.
14. R. R. Prabhu and M. A. Khadar, "Study of optical phonon modes of CdS nanoparticles using Raman spectroscopy," *Bulletin of Materials Science*, vol. 31, no. 3, pp. 511–515, 2008.
15. S. Velusamy, P. Vickraman and M. Jayachandran, "Structural and electrical studies of nano structured $Sn_{1-x}Sb_xO_2$ (x=0.0,1, 2.5, 4.5 and 7 at%) prepared by co-precipitation method," *Journal of Materials Science: Materials in Electronics*, vol. 21, no. 4, pp. 343-348, 2010.
16. A. K. Tripathi, M.C. Mathpal, P. Kumar, M. K. Singh, S. K. Mishra, R. K. Srivastava, J. S. Chung and G. Varma, "Photoluminescence and photoconductivity of Ni doped titania nanoparticles," *Advanced Materials Letters,* vol. 6, no. 3, pp. 201-208, 2015.
17. A. Maurya, P. Chauhan, S. K. Mishra and R. K. Srivastava, "Structural, optical and charge transport study of rutile TiO_2 nanocrystals at twocalcination temperatures," *Journal of Alloys and Compounds*, vol. 509, no. 33, pp. 8433-8440, 2011.
18. A. I. Kingon, J. P. Maria and S. K. Streiffer, "Review article Alternative dielectrics to silicon dioxide for memory and logic devices," Nature, vol. 406, pp. 1032-1038, 2000.
19. W. Li, C. Ni, H. Lin, C. P. Huang and S. I. Shah, "Size dependence of thermal stability of TiO_2 nanoparticles," *Journal of Applied Physics*, vol. 96, no. 11, pp. 6663-6668, 2004.

20. S.S. Mali, C.A. Betty, P.N. Bhosale and P. S. Patil, "Hydrothermal synthesis of rutile TiO_2 with hierarchical microspheres and their characterization," *Cryst Eng Comm*, vol. 13, pp. 6349-6351, 2011.
21. C. Rath, P. Mohanty, A. C. Pandey and N. C. Mishra, "Oxygen vacancy induced structural phase transformation in TiO_2 nanoparticles," *Journal of Physics D: Applied Physics*, vol. 42, pp. 205101-205106, 2009.
22. R. D. Shannon, "Phase Transformation Studies in TiO_2 Supporting Different Defect Mechanisms in Vacuum-Reduced and Hydrogen-Reduced Rutile," *Journal of Applied Physics*, vol. 35, no. 11, pp. 3414-3416, 1964.
23. H. L. Ma, J.Y. Yang, Y. Dai, Y.B.Zhang, B. Lu and G.H. Ma, "Raman study of phase transformation of TiO_2 rutile single crystal irradiation by infrared femtosecond laser," *Applied Surface Science*, vol. 253, pp. 7497-7500, 2007.
24. V.Swamy, A. Kuznetsov, L. S. Dubrovinsky, R. Caruso, D. Shchukin and B. Muddle, "Finite size and pressure effect on the Raman spectrum of nano crystalline anatse TiO_2," *Physics Review B*, vol. 71, pp. 184302-184310, 2005.
25. S. Mathew, A. K. Prasad, T. Benoy, P.P. Rakesh, M. Hari, T. M Libish, P. Radhakrishnan, V.P.N Nampoori and C.P.G. Vallabhan, "UV-Visible Photoluminescence of TiO_2 Nanoparticle prepared by Hydrothermal Method," *Journal of Fluorescence*, vol. 22, no. 6, pp. 1563-1569, 2012.

